3D Graphene: A Nanocarbon Innovation in Electrochemical Sensor Technology

Sahar Foroughirad, Behnaz Ranjbar, and Zahra Ranjbar

Abstract Nanocarbons, a diverse category of nanoscale carbon materials, have transformed scientific and industrial fields. Graphene, a remarkable nanocarbon, stands out due to its exceptional mechanical, electrical, and thermal properties. Three-dimensional (3D) graphene, with greater surface area and conductivity than its 2D counterpart, has gained recent popularity. In electrochemical sensing, the key component is the electrochemical electrode, driving chemical reduction reactions and generating signals. 3D graphene-based structures, featuring tailored meso- and micropores, offer interconnected hierarchical architectures, high surface area, intrinsic electrical conductivity, and a high signal-to-noise ratio, making them ideal electrochemical sensors. Two main fabrication strategies produce 3D graphene: 3D graphene aerogels and 3D graphene foams, each suited for different applications. Graphene foam's interconnected structure finds uses in electrochemical biosensors, adsorbents, supercapacitors, strain sensors, flexible electronics, space vehicle protection, EMI and microwave shielding, dampers, thermal interface materials, and flame-resistant materials. Incorporating nanomaterials like magnetite, doped elements, carbon nanotubes, and MXenes enhances these graphene-based structures. This chapter explores modification methods and applications of various 3D graphene-based structures as electrochemical sensors and offers insights into future synthesis and application prospects.

Keywords Nanocarbons · 3D graphene · Electrochemical sensor · Aerogel · Carbon nanotubes

S. Foroughirad
Faculty of Polymer Engineering, Sahand University of Technology, 51335-1996 Tabriz, Iran

Borna Chemi Arya Knowledge-Based Co., 5197817169 Tabriz, Iran

B. Ranjbar
Radsys Pooshesh Knowledge-Based Co, 1668836471 Tehran, Iran

Z. Ranjbar (✉)
Faculty of Surface Coating and Novel Technologies, Institute for Color Science and Technology, 1668836471 Tehran, Iran
e-mail: ranjbar@icrc.ac.ir

R. K. Gupta (ed.), *NanoCarbon: A Wonder Material for Energy Applications*,
Engineering Materials, https://doi.org/10.1007/978-981-99-9935-4_7

1 Introduction

Nanocarbons represent a diverse and fascinating class of carbon-based materials on the nanoscale. These materials, encompassing fullerenes, carbon nanotubes, graphene, and other carbon allotropes, have become a central focus in the field of nanotechnology. Their unique properties, such as high surface area, mechanical strength, and electrical conductivity, have paved the way for groundbreaking applications in various fields, including electronics, energy storage, and sensing. Among the various forms of nanocarbons, graphene has emerged as a particularly promising material. As a single layer of carbon atoms arranged in a two-dimensional honeycomb lattice, graphene exhibits high flexibility, remarkable electrochemical stability, significant specific surface area, and three-dimensional porosity, leading to high mass transfer rates and storage capacity [1]. Graphene-based nanomaterials can be synthesized in various dimensions, such as quantum dots (0D), nanofibers (1D), nanosheets (2D), and 3D stacks and gels with tailored properties. The pure graphene's thermal conductivity, attributed to its hole structure, sets it apart from other derivatives like graphene oxides. Classifying graphene as metal, semi-metal, or non-metal remains a challenge, but it best fits the semi-metal structure due to its low band gaps [2].

3D graphene nanostructures, a specific form of nanocarbon, have exceptional properties for application in electronic devices, overcoming drawbacks faced with other graphene-based materials. Issues such as low storage capacity, high agglomeration tendency in solvents, and the zero-gap nature of graphene as a semi-metal can be successfully addressed by employing 3D graphene structures [1]. The most common method for preparing 3D graphene involves stacking 2D graphene nanosheets. The resulting 3D graphene possesses low density, high mechanical and thermal properties, high specific surface area, and well-distributed porosity. Various types of 3D graphene structures, such as graphene foams, aerogels, and core–shell structures, have been developed according to research [2].

While the synthesis methods for 3D graphene structures are discussed in previous chapters, this chapter will focus on the applications of 3D graphene-based structures in fields like fuel cells, batteries, supercapacitors, biomedicals, separation, solar cells, etc. Specifically, we will review different components of an electrochemical sensor and their fabrication procedures, followed by the application of 3D graphene nanomaterials in electrochemical sensors. A detailed discussion will be provided on the related reaction mechanisms of 3D graphene nanostructures as a component in electrochemical sensors.

2 Electrochemical Sensors

The electrochemical sensing technique is remarkably considered a promising technique in sensor fabrications. Electrochemical sensors can be fabricated at low cost, with simple instruments and can provide rapid response, with high sensitivity and

selectivity. These sensors are capable of analyzing various species including organic/inorganic structures, metallic compounds, ions, and neutral species [3]. Conventional electrodes which were fabricated with no modifications, had many drawbacks in application. They showed no signals at low concentrations as they had low sensitivity and they usually displayed broad peak by which the analysis of samples with close potentials together, were almost impossible [4]. In the last decade, the modification of conventional electrodes put a spotlight on employing electrochemical sensing techniques as a promising candidate in various applications. The modifications are most often carried out by the incorporation of nanostructures into the as-prepared electrodes. These modified electrodes can possess fascinating characteristics such as high sensitivity and selectivity, low production cost, fast detection, and accurate quantification analysis of the target molecule [3]. Metallic nanowires, non-metallic nanomaterials, nanostructured polymers, carbon nanotubes, and graphene-based structures are the most applicable nanostructures in electrode modifications.

3 3D Graphene-Based Electrochemical Sensors

2D graphene structures, known as graphene nanosheets, are one of the hottest topics in the field of electrochemical sensing due to their characteristic properties. high specific surface area of about 2630 $m^2\ g^{-1}$, tremendous electrical conductivity of 200 S m^{-1}, mechanical and thermal durability, and good chemical resistance are some of the most critical properties of 2D graphene nanosheets [5]. However, some drawbacks were faced while employing 2D graphene structures. The high agglomeration tendency of the nanosheets is considered the most practical issue of these nanostructures. Due to π-π interactions, 2D nanosheets are highly attracted toward agglomeration which dramatically decreases the specific surface area and thus the electron transfer efficiency of the structure.

Fabrication of 3D graphene nanostructures can effectively overcome the aforementioned issue, leading to structures with high specific surface area and fascinating conductivity which facilitates electron transfer leading to quick and accurate sensing of the target molecule [6]. For example, El-Kady et al. [7], could prepare an electrode for the high specific surface area of 1520 $m^2\ g^{-1}$ with the aid of 3D graphene structures. For this purpose, they used the restacking technique as well as laser induction for reducing graphene and stacking them as a 3D structure. Moreover, Li et al. [8], could synergistically improve the electrode conductivity and capacity, by incorporating gold nanoparticles into the graphene network structure. The conductivity was reported to be enhanced by about two orders of magnitude, reaching more than 10^6 S m^{-1}. The graphene-based electrode sensitivity was reported to be improved by Araujo et al. [9]. The electrochemical sensor was employed for the detection of picric acid and the lowest detection limit for sensing was reported to be 0.48 mM. In another study, by Vanegas et al. [10], a novel electrochemical sensor was fabricated based on graphene structures for rapid, selective, and sensitive detection of biogenic amines. The detection limit was reported to be 11.6 μmol L^{-1} and the response

time was measured to be about 7 s which makes the prepared electrode a promising candidate for applications in rapid sensing technology.

3.1 Geometrical Classifications of 3D Graphene-Based Structures

The various 3D graphene nanostructures are classified into two major groups, in this chapter, regarding their chemical structures: (1) Solo 3D structures of graphene and (2) Their hybrid structures with other nanomaterials such as magnetite nanoparticles, carbon nanotubes, and other metallic or polymeric nanostructures. The subgroups are then separated according to the geometrical structure of the final 3D nanomaterial.

3.1.1 Solo 3D Structures of Graphene

The 3D graphene nanostructures can be classified into 2 main groups regarding their synthesis procedures. Randomly oriented 3D porous structures are mainly prepared by self-assembly technique and hierarchical structures in which uniform 3D structures such as foams and sponges are obtained by the templating approach.

3.1.2 Crumpled Ball Structures of 3D Graphene

Graphene-based 3D hydrogels and monoliths can be fabricated with the aid of self-assembly techniques, which include hydrothermal, laser engraving, and chemical reduction approaches. In all of these strategies, the graphene-based 2D structure is physically or chemically treated to be assembled and prepared 3D nanostructure based on graphene nanosheets [5, 11]. The physical treatment and graving of the surface with laser-based approaches are fully discussed by Vivaldi et al. [12]. The surface of the electrode can be engineered by adjusting the laser properties. The radiation of UV laser pulses onto the polymeric surfaces such as polyimide, induces a local heat of about 1700 ℃ as well as pressure up to 500 mJ cm^{-2}. The high temperature and pressure can effectively break the available aromatic structure bonds (C = O, C–N, C–H, and C–O bonds) and make new graphene-based structures followed by gas release. Moreover, metallic salts such as $FeCl_3$ can be added to the resin precursor, for obtaining a 3D graphene structure with good conductivity and high specific surface area [12]. Ball-shaped 3D structures of graphene are highly attractive as in this structure, graphene 2D nanosheets are assembled onto a specific core structure, which limits their further aggregation issues. Moreover, these porous 3D structures can provide abundant surfaces for ion and molecule transportation which is a critical point for applications of electrochemical-based sensing devices or storage systems. The obtained 3D graphene-based balls and spheres can be employed in

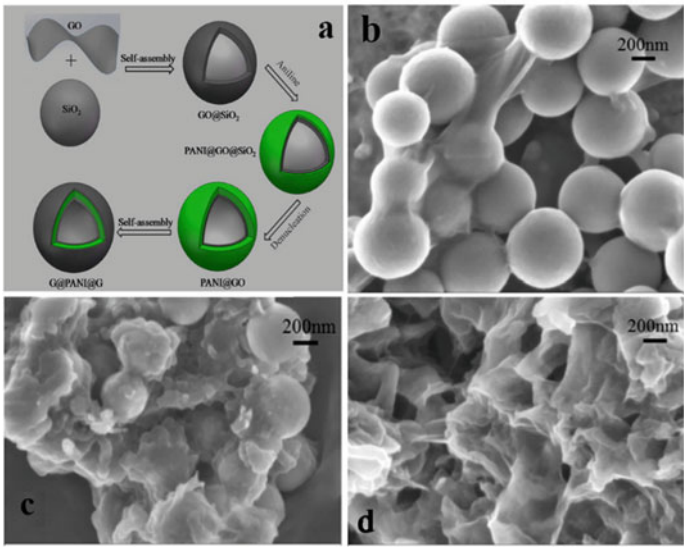

Fig. 1 **a** Schematic illustration of the synthesis procedure of G@PANI@G, SEM images of **b** GO@SiO_2, **c** PANI@GO@SiO_2 and **d** G@PANI@G. Adapted with permission [14], Copyright 2015, American Chemical Society

various devices in which the principal reactions are electrochemical ones including sensors, fuel cells, batteries, electrocatalytic reactions, etc. [13]. A robust ball-shaped core-double shell structure was reported by Liu et al. [14], the core and the outer shell were prepared with graphene, and the interlayer shell was designed to be polyaniline. The balls were prepared via a self-assembly approach. At first, GO@SiO_2 was synthesized by the Stober process, in the next step, surface modification was carried out to introduce amine to the surface of GO@SiO_2. The as-prepared polyaniline graphene oxide (denoted as PANI@GO) was added to the core mixture followed by the reduction of GO for obtaining G@PANI@G structure as represented in Fig. 1a. HF aqueous solution was employed for SiO_2 removal. SEM images at various stages of the fabrication are represented in Fig. 1b-d.

The obtained structure was reported to be resistant to shrinkage or swelling, with a high specific capacity of about 683 F g^{-1} and outstanding cycling stability of about 93% after 1000 cycles, making it a promising candidate for electrode applications.

3.1.3 Hierarchical Structures of 3D Graphene

On the other hand, hierarchical 3D graphene structures including foams and sponges are usually obtained via templating strategies. In this method, a specific template is chosen, polystyrene beads for instance, on top of which the assembly of graphene nanosheets is carried out. The process is continued by the elimination of the template

molecule, leading to a highly porous 3D structure based on graphene [15]. The template approach mainly consists of 3 main steps: (1) the graphene oxides are assembled on top of the chosen template; (2) the 3D graphene is produced on the template via various chemical approaches including chemical vapor deposition (CVD), (3) the elimination of the template will result in 3D graphene-based structure with high porosity and specific surface area. As a typical example in this regard, Zhu et al. [16], has recently reported the fabrication of 3D graphene electrode for application in lithium-ion batteries. For this purpose, the commercial Ni foam was washed thoroughly with deionized (DI) water and acetone. To remove the oxidized layer of the foam, it was heated up to 900 ºC under H_2 and Ar gases and then cooled down to the ambient temperature. The graphene layer was produced onto the treated Ni foam, via the CVD method. The 3D graphene foam was obtained by template removal. For this purpose, a diluted solution of nitric acid at about 45 ºC was prepared and the foam was immersed in it. The elimination of Ni resulted in soft 3D graphene foam. The Ni commercial foam was also employed for further treatment to make a 3D hierarchical graphene structure with nanoholes. The procedure was carried out with the aid of a self-made instrument which is fully discussed in the article. The obtained sensor was characterized, and its electrochemical behavior was fully investigated. The current density was set to be 200 mA g^{-1} and the cut-off voltage was 2 V. The discharge capacity for graphene Ni foam (denoted as G-NF) was measured to be 1700 mAh g^{-1}, which was much higher than Ni foam with no graphene coating. The bare graphene foam (GF) was obtained by the elimination of Ni. About 99.5% weight loss could make the free graphene foam, a promising candidate for applications in portable sensing devices. Moreover, by eliminating Ni, the inside pores of GF became accessible, leading to discharge capacity enhancement from 1700 mAh g^{-1} to 2800 mAh g^{-1}. From the obtained results, it was obvious that the increase in graphene surface can influence the electrochemical performance of the obtained cathode. For a deep insight into this phenomenon, a graphene foam with expanded surface area (E-GF) was prepared by making hierarchical pores into the Ni foam, and by making nanoholes into the graphene layers (P-E-GF). These two treatments could effectively enhance the surface area and thus the discharge capacity of the cathode to 4300 mAh g^{-1} and 7400 mAh g^{-1}, respectively.

3.1.4 Combined Strategies for Preparation of 3D Graphene

A new strategy based on the synergistic effect of self-assembly and templating was reported by Liu et al. [17]. In this article, a novel approach was introduced for the fabrication of graphene-based anode electrodes for Li and Na storage. For this purpose, the commercial Ni foam was immersed into the micro-sized GO suspension, followed by sonication for better diffusion of the suspension into the foam micropores. In the next step, the overnight dried foam was immersed into a specific mixture of nanosized GO and polystyrene beads with an average diameter of 0.5 μm. The etching procedure was then carried out to obtain free 3D graphene foam with graphene nanowires. The nanowires were obtained by self-assembly of nanosized

graphene onto the microsized interconnected graphene foam. Figure 2 represents the schematic illustration of the mentioned process as well as the SEM image of the prepared structure.

Electrochemical investigations were carried out to assess the quantitative performance of the prepared electrode. The results are represented in Fig. 3. The first discharge capacity of the anode was calculated to be 734.7 $mAhg^{-1}$ at the rate of 0.1 C (0.1 C = 37.2 $mAhg^{-1}$). The next charge capacity was reduced to 545.6 $mAhg^{-1}$, as a result of solid electrolyte interface layer formation. The reversible capacity of the 3D graphene hierarchical structure with nanowires (abbreviated as 3DGNW) was compared to that of the 3D porous graphene structure (abbreviated as 3DPG). The results revealed that the fabrication of a hierarchical 3D structure can increase the transportation of Li ions and thus enhance the anode performance. The cycling stability of 3DGNW showed an increase up to the 400th cycle which remained unchanged at about 467 $mAhg^{-1}$ during the next cycles to 1000 repeated cycles. The specific capacity was measured to increase continuously for 3DPG in all 1000 cycles. The increase in specific capacity during repeated cycles is a known phenomenon that is attributed to the formation of polymer film on top of the graphene surface. The results showed that this has no negative effect on the Li storage performance of the battery.

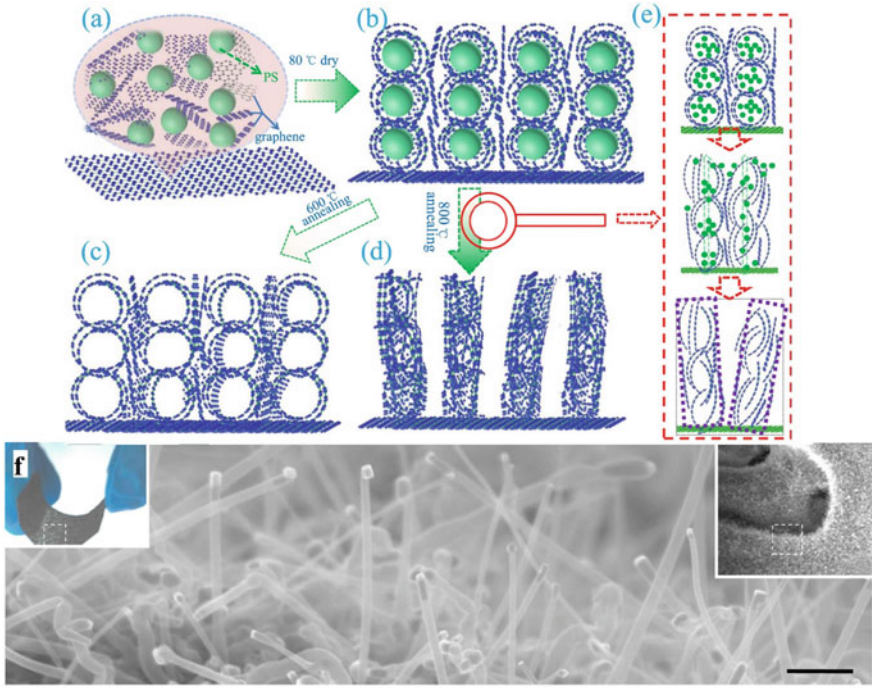

Fig. 2 Schematic representation of graphene nanowire fabrication. **a**–**e** and SEM image of 3D graphene nanowires **f**. Adapted with permission [17], Copyright 2017, Elsevier

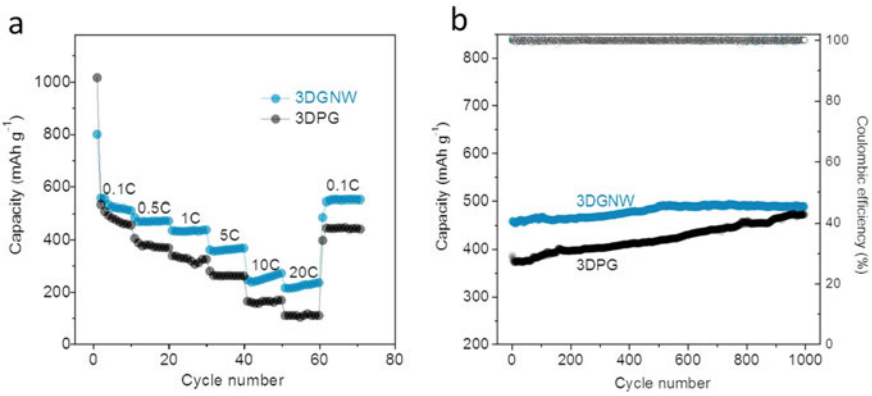

Fig. 3 lithium storage performance of 3D graphene nanowires. **a** Rate capability of 3DGNW and 3DPG at various C rates of 0.1, 1, 3, 5, 10, and 20 C. **b** Capacity retention of the 3DGNW and 3DPG electrodes at 1 C. Adapted with permission [17] Copyright 2017, Elsevier

3.2 Hybrid 3D Structures of Graphene

The functionality and chemical structure of the graphene nanostructures can be modified by incorporation of other nanostructures such as nanopolymers, iron oxide nanoparticles, carbon-based nanotubes, etc. This modification can be carried out during the reduction and assembly of the 2D nanosheets. this approach, simultaneous assembly and functionalization procedure, can result in functionalized hybrid hydrogels with fascinating properties [15]. The following will be a detailed discussion on modified graphene-based nanostructures.

3.3 Doped Structures of Graphene

Many elements such as Nitrogen and Boron and Cobalt are doped to graphene-based-3D nanostructures to enhance their catalytic and electrochemical performance. For instance, Jiang et al. [18], have synthesized graphene microspheres with hollow structures, in which Boron and Nitrogen were co-doped. The obtained structure was assessed for further application as an electrocatalyst of Oxygen Reduction Reactions (ORRs). The amino-modified SiO_2 nanoparticles with high porosity were employed as sacrificial templates. The GO was synthesized onto the surface of silica nanoparticles and then the homogeneous solution of NH_3BF_3 was added to the GO@SiO_2 core–shell structured mixture and the resultant suspension was hydrothermally treated for 12 h at 180 ºC. A further calcination procedure was carried out to enhance the conductivity of the samples. The obtained structure was immersed in HF solution for the illusion of the silica template. The electrochemical performance

of the hollow spheres was assessed by cyclic voltammetry. For assessing the reactivity of the samples toward O_2, the Oxygen or Nitrogen-saturated KOH solution with a concentration of 0.1 M was chosen. The difference between the two cyclic voltammetry curves of N_2 and O_2 suggested the specific attraction of the electrode toward oxygen. Other electrochemical analyses revealed that the obtained electrode can act more efficiently than the commercially available ones in ORRs. The N and B doped structures could enhance the adsorption of the Oxygen and the hollow structure provided higher available surface area to the electrolyte and thus reduce the overpotential of the ORRs. The fabricated electrode was reported to be a good candidate for further applications in fuel cells.

3.4 Graphene-Carbon Nanotube

Luo et al. [19], have recently reported the fabrication of a special 3D graphene structure, with a caterpillar shape, hybridized with carbon nanotubes (CNTs) to obtain a high-performance electrocatalyst. For this purpose, the 3D graphene oxide hydrogels with nanoscroll structure were obtained followed by the annealing at 750 ºC for obtaining 3D graphene nanoscrolls. After that, by introducing ethane gas to the mixture at the same temperature, the CNTs were prepared onto the 3D graphene structure via the CVD method. Co-$MoSe_2$-3D graphene@CNTs were prepared after that, with a facile solvothermal method. The various structures were denoted as Co–$MoSe_2$–GNS@CNT–y (y = 1, 2, 3, 4) according to the various amounts of $MoSe_2$, from about 71 wt% to 87 wt%, respectively. Moreover, various amounts of Co were doped onto the structure which was represented by zCo–$MoSe_2$–GNS@CNT (z = 1, 2, 3, 4) according to the Mo: Co molar ratios. For better attachment of Co-doped $MoSe_2$ onto the CNT brushes, Ni nanoparticles were employed and encapsulated into the tip of the CNT brushes. Figure 4 represents the schematic illustration of the step-by-step synthesis procedure and FESEM and TEM images of the 3D graphene-based nanostructure.

The goal of this research was to prepare a porous 3D structure for better electron transportation and the encapsulation of Ni nanoparticles could provide an effective surface for Co–$MoSe_2$ decoration and thus better electron traversing through CNTs resulting in lower catalytic energy barrier and more efficient hydrogen evolution reaction catalyst. Electrochemical investigations were carried out to assess the performance of the electrode kinetic and interface reactions., the Co–$MoSe_2$–GNS@CNT had the smallest Tafel slope, Fig. 5a, suggesting rapid discharge reaction in which the electrochemical desorption is the rate-limiting step. The hierarchical 3D graphene-based nanostructure was responsible for electron transfer rate enhancement. Moreover, the presence of 3D graphene@CNTs could increase the conductivity. The Co–$MoSe_2$-GNS@CNT nanocomposite showed the smallest semicircle in the Nyquist plots, Fig. 5b, with $R_{ct} = 3.2\ \Omega$. This reveals the facile charge transfer between the electrolyte and electrocatalyst interface which improves the rate of the reaction.

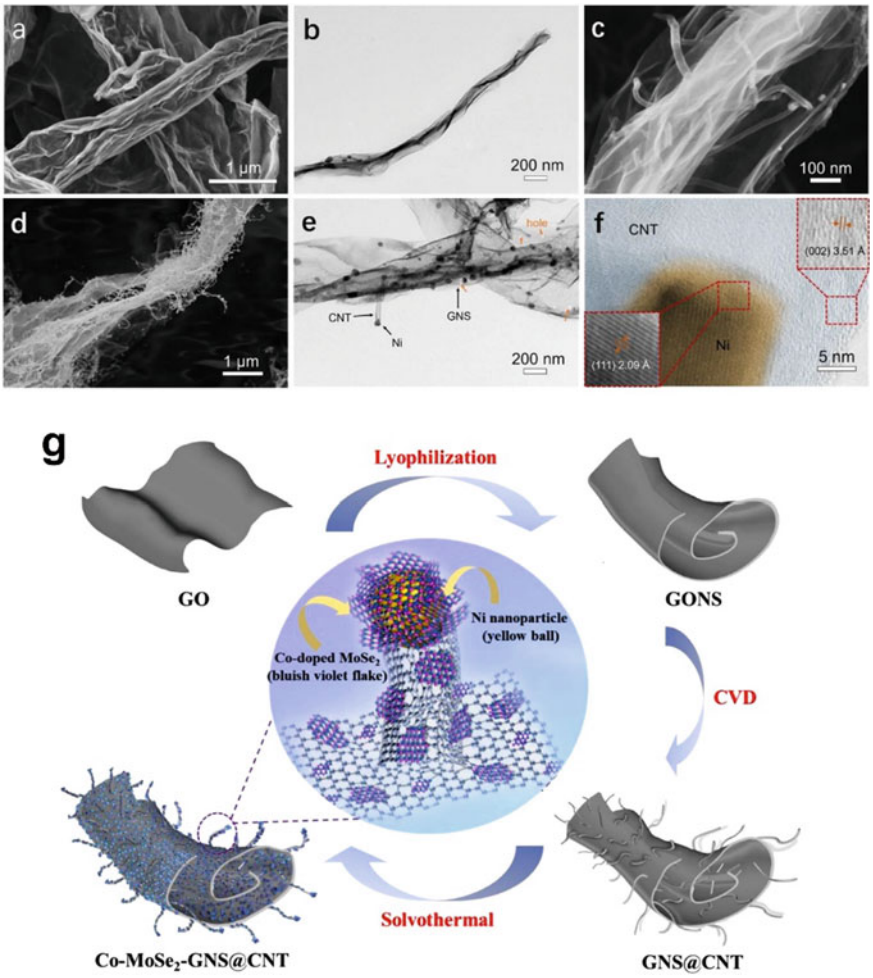

Fig. 4 TEM and FESEM images for: **a** and **b** GONS, **c**–**e** GNS@CNT, and HRTEM image of GNS@CNT. **g** Schematic illustration of the synthesis procedure for Co-$MoSe_2$-GNS@CNT. Adapted with permission [19], Copyright 2023, Elsevier

The unique 3D structure possessed excellent performance in both acidic and alkaline media, with high specific surface area with hierarchical pores which could effectively enhance the charge transfer and rate of the electrochemical reactions. This structure provided a new insight for preparing novel graphene-based-3D structures for electrochemical purposes including sensors and energy storage devices.

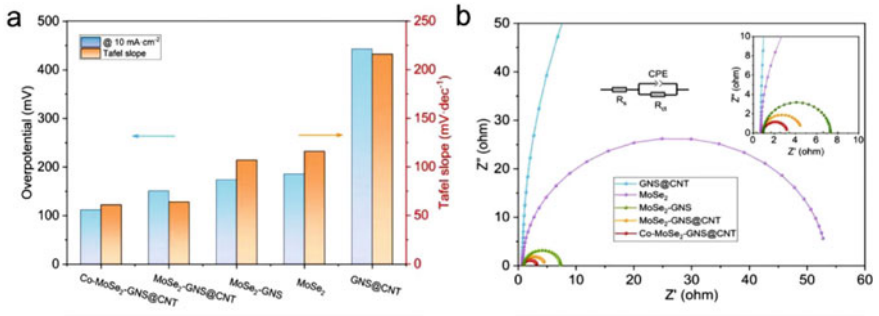

Fig. 5 **a** corresponding overpotential at 10 $mAcm^{-2}$ and value of the Tafel slope for different catalysts, **b** Nyquist plots. All measurements are in 0.5 mol L^{-1} H_2SO_4. Adapted with permission [19], Copyright 2023, Elsevier

3.5 Graphene–Fe_3O_4

The incorporation of magnetic nanoparticles into graphene-based systems is one of the hottest topics these days. Magnetic nanoparticles such as magnetite (Fe_3O_4) can be introduced into the graphene via two main methods: *in-situ* and ex-situ synthesis methods [20]. In the ex-situ method, the magnetite and the graphene-based structure are synthesized, separately, and then the final composite is prepared via mechanical mixing, solvothermal methods, or other grafting approaches. On the other hand, in the *in-situ* method, the magnetite nanoparticles are synthesized directly onto the graphene nanosheets, making a seeded nanosheet structure. In a typical example of an *in-situ* approach carried out by Cong et al. [21], ferrous ions were employed for the *in-situ* reduction of graphene oxide and then the Fe_3O_4 nanoparticles and α-FeOOH nanorods were directly synthesized onto the graphene nanosheets. In this study, $FeSO_4$ salt was added to the graphene oxide suspension at 90 ºC in an oil bath, after the first hour, the black floating resultant was observed which could be attributed to reduced graphene oxide. This was confirmed by XPS analysis in which the C–C bond peak was improved and the bonds containing O such as C = O and C-O were increased in intensity. With continuing the reaction, after 6 h, the black cylindrical hydrogel was prepared. The advantage of this method was that the scaling-up could be easily carried out resulting in the fabrication of 3D graphene hydrogel for further applications. In another study by Ershadi et al. [20], the ex-situ method was employed for the synthesis of amino-modified magnetite nanoparticles. The synthesized magnetic nanoparticles were then introduced to the 3D graphene framework. The results revealed that the electrodes based on magnetic 3D graphene have better electrochemical performance in comparison to bare Fe_3O_4 electrodes. Better nanoparticle distribution and less aggregation are responsible for this phenomenon. In this way, the rapid ion and electron transfer from GO to magnetite nanoparticles can increase the electrochemical performance, moreover, the higher porosity could be provided by the presence of magnetite nanoparticles leading to more surface of

contact between the electrolyte and the electrode and more available space for volume change in charge/discharge cycles.

Figure 6 represents the electrochemical performance of the optimum sample denoted as Fe_3O_4-E/rGO. The voltammograms of the sample at various rates and the calculation of the current constants are shown in Fig. 6a and b. The contribution for each supposed mechanism, diffusion-controlled reactions, and capacitive reactions, are calculated in Fig. 6c, and the percentage for each mechanism is measured, in Fig. 6d and e. At the cathode, reduction represented by peak A, about 90% of the produced current was due to the diffusion of the ions and the rest is provided by adsorption.

On the other hand, at the anode electrode, the oxidation denoted as peak B, especially at higher rates, the capacitive reactions become the most dominant mechanism leading to faster kinetic reaction in comparison to diffusion-controlled mechanism. The higher specific surface area and better porosity are responsible for this observation [20].

Zhao et al. [22], have reported the synthesis of hierarchical 3D structure based on magnetite nanoparticles and GO nanosheets. In this study, *in-situ* synthesis of Fe_3O_4 was carried out by which the magnetite nanoparticles were completely bonded to graphene oxide nanosheets, enhancing the specific surface area by mesoporous structure. The combination of magnetite mesoporous structure as well as macropores of rGO could synergistically improve the electrochemical performance of the composite. The specific capacity of the fabricated electrode was reported to be as

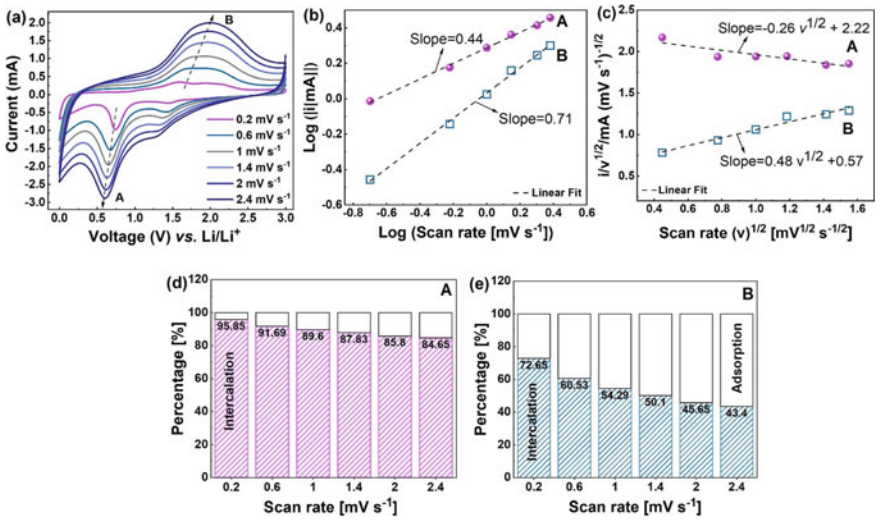

Fig. 6 **a** CV curves for Fe_3O_4-E/rGO sample at various rates, **b** log–log plot for reduction and oxidation current peaks specific rates, **c** $\sqrt{i/v}$ dependence on the square root of scan rate, **d** and **e** percentage contribution for each proposed mechanisms of capacitive and intercalation reactions. Adapted with permission [20], Copyright 2022, Elsevier

high as 551 mAh g^{-1} after 2000 repeated cycles at a current density of 2 A g^{-1}. Further investigations through the dominant mechanism revealed that the capacitive reactions are the most effective mechanism, leading to fast ion and charge transfer through the electrode, making this nanocomposite a promising candidate for applications in lithium-ion batteries. In another study by Tian et al. [23], a novel 3D structure of graphene-based magnetite aerogel was prepared and then employed for lithium-ion storage applications. The N-doped graphene aerogel nanocomposite, abbreviated as Fe_3O_4/NGA, was prepared through the following steps: (I) The commercially prepared GO was obtained and incorporated for the synthesis of the nanocomposite. (II) The iron (III) phthalocyanine (FePc) and GO were both dispersed in deionized water. The weight ratio of FePc: GO was set to be 1:1, 1:1.5, and 1: 2. The mixture was then heated at 180 ºC for 12 h during which the GO was reduced to rGO, the Fe_3O_4 nanoparticles were synthesized in situ and the N element which was present in the phthalocyanine was assembled onto the rGO to make Fe_3O_4/N-doped rGO aerogel. (II) For improved electrochemical performance, further annealing was carried out at 700 ºC for three hours. The obtained 3D structure was employed as an anode electrode in lithium-ion batteries. The optimized sample, with a FePc: GO ratio of 1:1.5, revealed outstanding electrochemical performance and cyclic stability with a specific capacity of about 1185 mAh g^{-1} at a current density of 1 A g^{-1} after 500 continuous charge/discharge cycles.

There are many similar studies in which the graphene oxide properties are improved by the incorporation of magnetite nanoparticles onto the graphene aerogel. Other properties rather than electrochemical performance can be thermal, mechanical, catalytic, etc. Jalaly et al. [24], could improve the thermal and mechanical performance of 3D graphene-based structures by introducing Fe_3O_4 nanoparticles into the system. Magnetite nanoparticles at various contents, 0–30 wt.%, were encapsulated into graphene nanosheets via the ex-situ method. The compressive strength of 6.85 kPa could be obtained at 20 wt.% of Fe_3O_4 and the best mechanical strength was obtained at 10 wt.% of Fe_3O_4. Liu et al. [25], could also report the successful synthesis of 3D graphene structure with magnetite incorporation, for better catalytic performance. Highly active Fe_3O_4 sites could effectively improve charge and mass transfer through the composite. The most applicable achievement of this research was limiting the metal-leaching issue which was faced when metal–organic frameworks are employed.

3.6 Graphene-MXene

MXenes, as a two–dimensional material, have recently attracted a lot of interest because of their unique electrical, chemical, and physical properties such as high hydrophilicity, thermal stability, surface area, and electrical conductivities, being environmentally friendly and unique layered morphology. Due to these characteristics, they are appropriate for electronic applications, catalysis, and energy storage devices. Their structure contains carbonitrides, nitrides, or metal carbides which

are added to two-dimensional nanomaterials groups. MXenes general formula is $M_{n+1}X_nT_x$, i.e., n is an integer between 1–3 and T is surface functional groups (–F, –OH and = O). In MXene, M represents various transition metals like Mo, Cr, Nb, Ti, Sc, V, etc., and X represents nitrogen and/or carbon. Calcination and alkalization treatment can also be carried out to make changes to the functional groups based on the nature of the application. The number of MXenes is being expanded with increasing various synthetic methods and they are highly employed for fabrication of hybrid 3D graphene-based nanostructures. Gu et al. [26], synthesized a three-dimensional hybrid film based on graphene and MXene ($Ti_3C_2T_x$) via a simple mixing drying technique as an electrochemical biosensor to be used in glucose sensing. The pore size is an important parameter for immobilizing the enzymes and of course biosensing performance. They tuned the internal pore sizes by changing in MXene and graphene ratios. The more graphene content, the more porous the structure. It was shown that the 1:2 and 1:3 ratio in MXene: graphene showed better sensing results. In another research work, Feng et al. [27], also made a three-dimensional glucose sensor based on graphene, $Ti_3C_2T_x$ MXene, and gold nanoparticles. They used self-reduction and mixing-freeze-drying methods to build a carrier for the immobilization of glucose oxides for better sensing efficiency. As we mentioned before, the pore size has a great influence on sensing performance. Just like Gu et al. [26], they also controlled the pore's structure by changing the MXene to graphene ratio. Adding gold nanoparticles can reduce the redox potential and increase the electron transport efficiency along with the porous sensor structure. The sensor they made showed a good and repeatable sensitivity at 2 μM until 0.4 mM glucose concentration equal to 169.49 $\mu A/(mM \cdot cm^2)$. This sensor can be potentially applied in biochemistry, drug analysis, and clinical diagnostics. Ma et al. [28], made a highly conductive porous aerogel material based on reduced graphene oxide and MXene. These two important properties made the composite a good candidate to be used as a pressure sensor. The sensor they made showed high repeatability over 10,000 times, below 200-ms response, and high sensitivity around 22.5 kPa^{-1}. A Ti_3C_2 MXene/graphene oxide nanocomposite was synthesized by Zheng et al. [29]. They applied this nanocomposite for making inkjet-printed hydrogen peroxide biosensors. They showed that their printable nanocomposite showed outstanding electrochemical sensing properties.

In another research work, Xie et al. [30], made an electrochemical sensor based on MXene and reduced graphene oxide (rGO) for carbendazim sensing. They used rGO to enhance the sensing performance of MXene. Carbendazim or methylbenzimidazol-2-ylcarbamate is a broad-spectrum benzimidazole fungicide and can be considered a toxic material. This material is widely utilized in seed, soil, and foliar treatment. It could be harmful to human health even in low amounts. Accordingly, the determination of carbendazim in vegetables and fruits is very important. The authors showed that MXene/graphene composite can be used as a reliable candidate as a carbendazim sensor. They utilized graphene as spacers in MXene sheets. Graphene spacers isolate the sheets and prevent them from restacking leading to an elevation in the interlayer spacing between MXene layers. It leads to an increase in structural robustness, electrical conductivity, and specific capacities.

The MXene nanosheet which is a water-soluble two-dimensional substrate inhibits graphene aggregation. The sensor that they made showed a low limit of detection (LOD) of about 0.67 nm and a linear and wide sensing range between 2 nm and 10 μm. They checked their laboratory outcomes with the actual orange juice and cucumber samples and got reliable results. Aziz et al. [31], reviewed the effect of wearable sensors based on graphene and MXene on the environment. Because of their high electrocatalytic activity and surface area, they can be utilized in biochemical and biophysical sensors. They mentioned that although MXene and graphene have perfect sensing performance, their environmental impacts, biological toxicity, and biocompatibility need more investigation, especially in in-vivo studies.

Wang et al. [32], who proposed a roadmap for the future of MXene-based materials, introduced graphene/MXene composite, a candidate to be used in biosensors. On the other hand, Mostafavi et al. [33], specially reviewed the applications of MXene/graphene in biomedical and electrochemical biosensors. They believed that these kinds of sensors show low detection limit, fast response time (just about 15 ms to be recovered), high stability and performance. Liu et al. [33], synthesized a three-dimensional aerogel based on MXene/rGO/SnO_2 by the hydrothermal process as an electrochemical sensor for the detection of formaldehyde. The sensor they made showed perfect reversibility, fast response/recovery rate, good selectivity, and linearity between 10 and 200 ppm. They attribute the high sensing efficiency to the presence of p-n junctions, their composition, and their special three-dimensional structure. Wang et al. [33], have recently made a flexible three-dimensional electrochemical sample based on MXene and graphene for sensing uric acid, dopamine, and ascorbic acid. They showed the proposed sensor could mention the amount of uric acid, dopamine, and ascorbic acid precisely with no overlap. Furthermore, it showed a good approach for the wearable continuous yet non-invasive monitoring system for human well-being. It is also washable-free, user-friendly, and skin-adaptable.

4 Future Perspective of 3D Graphene-Based Sensors

Electrochemical-based electrodes are highly employed in various fields including, energy storage devices, selective adsorption of analytes, fuel cells, etc. for assuring accurate measurement, traditional electrochemical sensors require the attachment and immobilization of the eluent, or analyte, to the surface of the electrode. This was time-consuming, and limited the activity of the analytes, specifically when the adsorbate was a bio-based species and also the reusability of the electrode was dramatically affected. New strategies are recently emerged in electrode fabrication, in which there is no need for the adsorbate to be immobilized. Homogeneous electrochemical sensors (HESs) are a new class of sensors in which there is no need for immobilization of the analyte [34].

HESs are a subcategory of electrochemical sensors that the accurate detection of the analyte quantity can be accrued with no immobilization. This detection lies on many strategies such as the change in configuration of the electroactive dye which

is attached to the electrode [35, 36], intercalation of the attached dyes [37], or the controlled release of the attached dyes into the homogeneous media by which high effective and accurate probe electrode can be fabricated for highly sensitive detection of analytes [38]. The aforementioned technique is a promising one for the fabrication of electrochemical sensors, for the detection of various analytes. The approach is facile, cost-effective, fast, and accurate, however, there is just a limited number of research that focused on this method, during the past few years. Homogeneous electrodes are fabricated for the detection of inhibitors [39], pesticides [40], heavy metal ions [41], antibiotics [42], and biomarkers [43]. Many strategies and applications were discussed in this chapter, for the synthesis and application of 3D graphene-based nanostructures, however, no research could be found on incorporation of 3D graphene-based structures in immobilized-free electrodes. Moreover, it seems that there is a gap in the fabrication of HESs for applications in fuel cells, batteries, and other storage devices. By employing the free-immobilization technique in the fabrication of 3D graphene-based electrodes, novel and highly effective electrochemical-based- based electrodes can be fabricated, which can open a new insight into the world of electrochemical sensors.

5 Conclusion

Exceptional properties such as electrical, mechanical, and thermal properties have put graphene under the spotlight of research. Compared with two-dimensional graphene-based materials, three-dimensional graphene-based structures have a more specific surface area and higher porosity, which means that more target molecules can be loaded onto the structure. Moreover, many factors such as contact resistance, aggregation, and restacking tendency can be controlled in 3D graphene leading to higher electrical conductivity in application. Electrode, as a critical part of the sensing system in electrochemical sensors, can be designed with the aid of 3D graphene-based nanostructures. For this purpose, a tailor-made architecture of 3D graphene with interconnected mesopores and micropores is incorporated into the electrode fabrication. The obtained electrode is reported to have outstanding properties including, high surface area, fast kinetic and mass transportation, intrinsic electrical conductivity, high sensitivity and selectivity, etc. making them a promising candidate for applications in various fields such as solar cells, storage devices, separation, biomedical and electrochemical sensors. Two main categories of 3D graphene structures are fully discussed in the chapter 3D structures which are prepared by self-assembly of graphene nanosheets, and hierarchical structures by which graphene-based foams and sponges are fabricated. Each aforementioned structure has its application, for example, foams and sponges are widely used in adsorbents, biosensing materials, flexible sensors, super-capacitors, strain sensors, aerospace vehicles, and flame-resistant materials. Various nanomaterials can be incorporated into the 3D graphene frameworks to enhance their properties. These nanomaterials can be named magnetite nanoparticles, carbon nanotubes, MXenes, and doped structures of graphene. By fabrication

of these hybrid structures, many new properties, such as magnetic response, can be introduced to the system. Moreover, already existing features such as mechanical and electrical conductivity, can be remarkably improved. This can guarantee the performance of the fabricated electrode in electrochemical sensing devices. In this chapter, we discussed strategies for the fabrication of various hybrid structures of 3D graphene-based nanomaterials, and some of the most highlighted research in each category were included for better insight. At the end, we took a look into the future perspective of electrochemical sensing materials and their new potentials, in synthesis and applications.

References

1. Wang, H., Yuan, X., Zeng, G., Wu, Y., Liu, Y., Jiang, Q., Gu, S.: Three-dimensional graphene-based materials: Synthesis and applications from energy storage and conversion to electrochemical sensor and environmental remediation. Adv. Colloid Interface Sci. **221**, 41–59 (2015)
2. Makwana, M.V., Patel, A.M.: Recent Applications and Synthesis Techniques of Graphene. Micro Nanosyst. **14**(4), 287–303 (2022)
3. Asadian, E., Ghalkhani, M., Shahrokhian, S.: Electrochemical sensing based on carbon nanoparticles: A review. Sensors Actuators, B Chem. **293**(April), 183–209 (2019)
4. Baig, N., Sajid, M., Saleh, T.A.: "Recent trends in nanomaterial-modified electrodes for electroanalytical applications", TrAC -. Trends Anal. Chem. **111**, 47–61 (2019)
5. Lu, L.: Recent advances in the synthesis of three-dimensional porous graphene and its applications in the construction of electrochemical (bio)sensors for small biomolecule detection. Biosens. Bioelectron. **110**(March), 180–192 (2018)
6. Xu, J., Wang, Y., Hu, S.: Nanocomposites of graphene and graphene oxides: Synthesis, molecular functionalization and application in electrochemical sensors and biosensors. A review. Microchim. Acta **184**(1), 1–44 (2017)
7. El-Kady, M.F., Strong, V., Dubin, S., Kaner, R.B.: Laser scribing of high-performance and flexible graphene-based electrochemical capacitors. Science (80-.). **335**(6074), pp. 1326–1330 (2012)
8. Li, R.Z., Peng, R., Kihm, K.D., Bai, S., Bridges, D., Tumuluri, U., Wu, Z., Zhang, T., Compagnini, G., Feng, Z., Hu, A.: High-rate in-plane micro-supercapacitors scribed onto photo paper using: In situ femtolaser-reduced graphene oxide/Au nanoparticle microelectrodes. Energy Environ. Sci. **9**(4), 1458–1467 (2016)
9. de Araujo, W.R., Frasson, C.M.R., Ameku, W.A., Silva, J.R., Angnes, L., Paixão, T.R.L.C.: Single-Step reagentless laser scribing fabrication of electrochemical Paper-Based analytical devices. Angew. Chemie - Int. Ed. **56**(47), 15113–15117 (2017)
10. Vanegas, D.C., Patiño, L., Mendez, C., de Oliveira, D.A., Torres, A.M., Gomes, C.L., McLamore, E.S.: Laser scribed graphene biosensor for detection of biogenic amines in food samples using locally sourced materials. Biosensors **8**(2), 42 (2018)
11. Tehrani, F., Bavarian, B.: Facile and scalable disposable sensor based on laser engraved graphene for electrochemical detection of glucose. Sci. Rep. **6**(June), 1–10 (2016)
12. Vivaldi, F.M., Dallinger, A., Bonini, A., Poma, N., Sembranti, L., Biagini, D., Salvo, P., Greco, F., Di Francesco, F.: Three-Dimensional (3D) Laser-Induced graphene: structure, properties, and application to chemical sensing. ACS Appl. Mater. Interfaces **13**(26), 30245–30260 (2021)
13. Nazarian-Samani, M., Kim, H.K., Park, S.H., Youn, H.C., Mhamane, D., Lee, S.W., Kim, M.S., Jeong, J.H., Haghighat-Shishavan, S., Roh, K.C., Kashani-Bozorg, S.F., Kim, K.B.: Three-dimensional graphene-based spheres and crumpled balls: Micro- and nano-structures, synthesis strategies, properties and applications. RSC Adv. **6**(56), 50941–50967 (2016)

14. Liu, X., Wen, N., Wang, X., Zheng, Y.: A High-performance hierarchical graphene@polyaniline@graphene sandwich containing hollow structures for supercapacitor electrodes. ACS Sustain. Chem. Eng. **3**(3), 475–482 (2015)
15. Li, C., Shi, G.: Three-dimensional graphene architectures. Nanoscale **4**(18), 5549–5563 (2012)
16. Zhu, X., Wu, Y., Wang, Z., Wang, Y., Man, Z., Wen, X., Lv, Z., Wang, X.: Hierarchical architecture: A novel, facile and cost-efficient strategy to boost electrochemical performance of Li-O2 battery cathodes. Chem. Eng. J. **450**(P4), 138462 (2022)
17. Liu, X., Chao, D., Su, D., Liu, S., Chen, L., Chi, C., Lin, J., Shen, Z.X., Zhao, J., Mai, L., Li, Y.: Graphene nanowires anchored to 3D graphene foam via self-assembly for high performance Li and Na ion storage. Nano Energy **37**(February), 108–117 (2017)
18. Jiang, Z., Zhao, X., Tian, X., Luo, L., Fang, J., Gao, H., Jiang, Z.J.: Hydrothermal synthesis of boron and nitrogen codoped hollow graphene microspheres with enhanced electrocatalytic activity for oxygen reduction reaction. ACS Appl. Mater. Interfaces **7**(34), 19398–19407 (2015)
19. Luo, H., Gao, H., Zhang, X., Yang, F., Liu, C., Xu, K., Guo, D.: Caterpillar-like 3D graphene nanoscrolls@CNTs hybrids decorated with Co-doped $MoSe_2$ nanosheets for electrocatalytic hydrogen evolution. J. Mater. Sci. Technol. **136**, 43–53 (2023)
20. Ershadi, M., Javanbakht, M., Brandell, D., Ahmad Mozaffari, S., Molaei Aghdam, A.: Facile Synthesis of Amino-functionalized Mesoporous Fe_3O_4/rGO 3D Nanocomposite by Diamine compounds as Li-ion Battery Anodes. Appl. Surf. Sci., **601**, p. 154120 (2022)
21. Cong, H.P., Ren, X.C., Wang, P., Yu, S.H.: Macroscopic multifunctional graphene-based hydrogels and aerogels by a metal ion induced self-assembly process. ACS Nano **6**(3), 2693–2703 (2012)
22. Zhao, P., Jiang, L., Li, P., Xiong, B., Zhou, N., Liu, C., Jia, J., Ma, G., Zhang, M.: Tailored engineering of Fe_3O_4 and reduced graphene oxide coupled architecture to realize the full potential as electrode materials for lithium-ion batteries. J. Colloid Interface Sci. **634**, 737–746 (2023)
23. Tian, L., Xie, Y., Lu, J., Hu, Q., Xiao, Y., Liu, T., Davronbek, B., Zhu, X., Su, X.: Self-assembled 3D Fe_3O_4/N-Doped graphene aerogel composite for large and fast lithium storage with an excellent cycle performance. J. Electroanal. Chem. **922**(June), 116763 (2022)
24. Jalaly, M., Hosseini, R., Bakhshi, A., Chehelamirani, M.: Self-assembly synthesis of 3D graphene/nano-Fe_3O_4 hybrid aerogels with improved mechanical and thermal properties. J. Alloys Compd. **902**, 163718 (2022)
25. Liu, M., Liu, Y., Liu, X., Chu, C., Yao, D., Mao, S.: Peroxydisulfate activation by 2D MOF-derived Ni/Fe_3O_4 nanoparticles decorated in 3D graphene oxide network. Sep. Purif. Technol. **301**(May), 121967 (2022)
26. Gu, H., Xing, Y., Xiong, P., Tang, H., Li, C., Chen, S., Zeng, R., Han, K., Shi, G.: Three-Dimensional porous $Ti_3C_2T_x$ MXene–Graphene hybrid films for glucose biosensing. ACS Appl. Nano Mater. **2**(10), 6537–6545 (2019)
27. Feng, L., Qin, W., Wang, Y., Gu, C., Li, X., Chen, J., Chen, J., Qiao, H., Yang, M., Tian, Z., Yin, S.: $Ti_3C_2T_x$ MXene/Graphene/AuNPs 3D porous composites for high sensitivity and fast response glucose biosensing. Microchem. J. **184**, 108142 (2023)
28. Ma, Y., Yue, Y., Zhang, H., Cheng, F., Zhao, W., Rao, J., Luo, S., Wang, J., Jiang, X., Liu, Z., Liu, N., Gao, Y.: 3D synergistical MXene/Reduced graphene Oxide aerogel for a piezoresistive sensor. ACS Nano **12**(4), 3209–3216 (2018)
29. Zheng, J., Diao, J., Jin, Y., Ding, A., Wang, B., Wu, L., Weng, B., Chen, J.: An inkjet printed Ti3C2-GO electrode for the electrochemical sensing of hydrogen peroxide. J. Electrochem. Soc. **165**(5), B227 (2018)
30. Xie, Y., Gao, F., Tu, X., Ma, X., Xu, Q., Dai, R., Huang, X., Yu, Y., Lu, L.: Facile synthesis of MXene/Electrochemically reduced graphene oxide composites and their application for electrochemical sensing of carbendazim. J. Electrochem. Soc. **166**(16), B1673 (2019)
31. Aziz, A., Asif, M., Ashraf, G., Iftikhar, T., Hussain, W., Wang, S.: Environmental significance of wearable sensors based on MXene and graphene. Trends Environ. Anal. Chem. **36**, e00180 (2022)

32. Wang, Q., Han, N., Shen, Z., Li, X., Chen, Z., Cao, Y., Si, W., Wang, F., Ni, B.-J., Thakur, V.K.: MXene-based electrochemical (bio) sensors for sustainable applications: Roadmap for future advanced materials. Nano Mater. Sci. **5**(1), 39–52 (2022)
33. Mostafavi, E., Iravani, S.: MXene-Graphene composites: a perspective on biomedical potentials. Nano-Micro Lett. **14**(1), 130 (2022)
34. Li, H., Qi, H., Chang, J., Gai, P., Li, F.: Recent progress in homogeneous electrochemical sensors and their designs and applications. TrAC - Trends Anal. Chem. **156**, 116712 (2022)
35. Feng, Z., Zhao, R.J., Lu, Z.H., Jia, L.P., Ma, R.N., Zhang, W., Shang, L., Xue, Q.W., Wang, H.S.: Construction of aptasensors for sensitive detection of 8-OH-dG based on a diffusion mediated electrochemiluminescence quenching effect. Chem. Commun. **56**(75), 11074–11077 (2020)
36. Ni, J., Lin, H., Yang, W., Liao, Y., Wang, Q., Luo, F., Guo, L., Qiu, B., Lin, Z.: Homogeneous electrochemiluminescence biosensor for the detection of RNase a activity and its inhibitor. Anal. Chem. **91**(22), 14751–14756 (2019)
37. Zhang, J., Wu, D.Z., Cai, S.X., Chen, M., Xia, Y.K., Wu, F., Chen, J.H.: An immobilization-free electrochemical impedance biosensor based on duplex-specific nuclease assisted target recycling for amplified detection of microRNA. Biosens. Bioelectron. **75**, 452–457 (2016)
38. Huang, X., Bian, X., Chen, L., Guo, L., Qiu, B., Lin, Z.: Highly Sensitive homogeneous electrochemiluminescence biosensor for alkaline phosphatase detection based on Click Chemistry-Triggered branched hybridization chain reaction. Anal. Chem. **93**(29), 10351–10357 (2021)
39. Ge, L., Hong, Q., Li, H., Li, F.: A laser-induced TiO2-decorated graphene photoelectrode for sensitive photoelectrochemical biosensing. Chem. Commun. **55**(34), 4945–4948 (2019)
40. Qi, H., Li, H., Li, F.: Aptamer Recognition-Driven homogeneous electrochemical strategy for simultaneous analysis of multiple pesticides without interference of color and fluorescence. Anal. Chem. **93**(21), 7739–7745 (2021)
41. Ge, L., Hong, Q., Li, H., Liu, C., Li, F.: Direct-Laser-Writing of metal Sulfide-Graphene nanocomposite photoelectrode toward sensitive photoelectrochemical sensing. Adv. Funct. Mater. **29**(38), 1–10 (2019)
42. Wang, X., Dong, S., Gai, P., Duan, R., Li, F.: Highly sensitive homogeneous electrochemical aptasensor for antibiotic residues detection based on dual recycling amplification strategy. Biosens. Bioelectron. **82**, 49–54 (2016)
43. Chang, J., Wang, X., Wang, J., Li, H., Li, F.: Nucleic Acid-Functionalized Metal-Organic framework-based homogeneous electrochemical biosensor for simultaneous detection of multiple tumor biomarkers. Anal. Chem. **91**(5), 3604–3610 (2019)